

# INFORMATION TECHNOLOGY. AUTOMATION

## ІНФОРМАЦІЙНІ ТЕХНОЛОГІЇ. АВТОМАТИЗАЦІЯ

UDC 621.341.572

V. Tigariev, PhD, Assoc. Prof.,

O. Lopakov,

V. Kosmachevskiy,

O. Andriianov, PhD, Assoc. Prof.

Odessa Polytechnic National University, 1 Shevchenko Ave., Odesa, Ukraine, 65044; e-mail: kedrodessa9@gmail.com

## ALGORITHM FOR ONLINE COEFFICIENT CORRECTION

### ARTIFICIAL NEURAL NETWORK IN MPPT

### CONTROLLERS FOR SOLAR BATTERIES

*V. Tigariev, A. Lopakov, V. Kosmachevskiy, O. Andriianov.* Алгоритм онлайн-корекції коефіцієнтів штучної нейронної мережі MPPT-контролерів сонячних батарей. Основним елементом сонячних енергетичних установок зазвичай є силовий каскад (DC/DC – перетворювач, інвертор). Перетворювачі у таких системах генерування повинні мати високий ККД (не менше 90%), високу якість вихідного сигналу та забезпечувати роботу енергоустановки з максимальним відбором потужності від сонячної батареї. Характеристики сонячних батарей суттєво залежать від погодних умов, таких як освітленість та температура. Протягом дня температура та потужність опромінення сонячного генератора постійно змінюються. Ці зміни призводять до зсуву точки максимальної потужності та до часткової втрати потужності установки. Щоб забезпечити отримання максимально можливої потужності від сонячної батареї, необхідно використовувати відповідний алгоритм відстеження точки максимальної потужності (MPPT). Для MPPT застосовуються спеціалізовані контролери, які використовують один із алгоритмів для оптимізації робочої точки фотомодулів. Найчастіше використовували методи: обурення та спостереження, метод зростаючої провідності, метод постійної напруги. Метод відстеження точки максимальної потужності, що використовується, багато в чому визначатиме ефективність фотоелектричної системи генерування. Максимальний вибір потужності від сонячних батарей можливий лише при здійсненні безперервного регулювання напруги батареї в оптимальній робочій точці. Таким чином, при проектуванні та створенні сучасних ефективних фотоелектричних систем генерування повинні вирішуватись завдання не лише покращення технології сонячних елементів з підвищенням ККД, а й низка питань проектування фотоелектричних перетворювачів та їх системи управління з метою суттєвого підвищення їх енергетичної ефективності.

*Ключові слова:* штучна нейронна мережа, вольт-амперна характеристика (ВАХ), вольт-ватна характеристика (ВВХ), Light induced degradation (LID), Potential induced degradation (PID), система управління, сонячна батарея, відстеження точки максимальної потужності (MPPT)

*V. Tigariev, A. Lopakov, V. Kosmachevskiy, O. Andriianov.* Algorithm for online coefficient correction artificial neural network in MPPT controllers for solar batteries. The main element of solar power plants is usually a power cascade (DC/DC converter, inverter). Converters in such generation systems should have high efficiency (at least 90%), high output signal quality and ensure operation of the power plant with maximum selection of power from the solar battery. The characteristics of solar panels depend heavily on weather conditions such as light and temperature. During the day, the temperature and power of the solar generator are constantly changing. These changes result in a shift in the maximum power point and a partial loss of power. In order to obtain the maximum possible power from the solar battery, it is necessary to use the appropriate maximum power point tracking algorithm (MPPT). For MPPT, specialized controllers are used, which use one of the algorithms to optimize the working point of the photomodels. The most commonly used methods are perturbation and observation, increasing conductivity, constant voltage. The maximum power point tracking method used will largely determine the efficiency of the photovoltaic generation system. Maximum power recovery from solar panels is possible only when the battery voltage is continuously regulated at an optimal operating point. Thus, the design and development of modern efficient photovoltaic generation systems should address not only the improvement of high efficiency solar cell technology, but also a number of issues of designing photovoltaic converters and their control systems to significantly improve their energy efficiency.

*Keywords:* Artificial Neural Network, Volt-Ampere Characteristic (VAC), Volt-Watt Characteristic (VWC), Induced Degradation (LID), Potential Degradation (PID), Control System, Solar Battery, Maximum Power Point Tracking (MPPT)

### 1. Introduction

To achieve the goal of improving energy efficiency, the converters used in photovoltaic power plants should have a control system based on the maximum power point tracking algorithm, which will be the key to maximizing the efficiency of the solar system. In foreign literature, the algorithm is better known as Maximum Power Point Tracking (MPPT). For MPPT are used specialized controllers, which use one of the algorithms to optimize the solar operating point. The design and development of modern, efficient photovoltaic systems should therefore address the development of an appropriate

DOI: 10.15276/opus.2.68.2023.09

© 2023 The Authors. This is an open access article under the CC BY license (<http://creativecommons.org/licenses/by/4.0/>).

control system. The transition to solar cell power point control is a modern trend in photovoltaic generation.

## 2. Analysis of literature data and problem statement

Widely known works on MPPT authors such as Hohm, D.P., Esmar, T., Chapman, P.L., Femia, N., Petrone, G., Spagnuolo, G., Vitelli, M. and etc. But classical analog algorithms are not the best solution for the MPPT problem, despite their obvious advantages. These algorithms are quite slow to reach the maximum power point and are limited in accuracy of operation. To achieve higher accuracy, algorithms are subject to different modifications, but their dynamic characteristics are impaired. Controllers are used to track the maximum power point, which use one of the algorithms to optimize the photomodule operating point [1, 2, 3–7]. To date, many different algorithms have been developed to track the maximum power point. Each method has its advantages and disadvantages. Classical algorithms cannot find a high-speed maximum power point, it requires many iterations. Consequently, the task of tracking the maximum power point is still relevant.

Currently, research into the possibilities of artificial neural networks (ANN) and their expansion is a priority for many researchers. The ANN provides an alternative way to solve complex problems. A neural network, with the right structure, can compute the values of any continuous function with some predetermined accuracy. The neural network does not require knowledge of the internal parameters of the solar module; it learns quickly, it has the ability to optimize and approximate. Hence, the use of ANN to track the maximum power point is relevant and of practical and scientific importance.

## 3. The purpose and objectives of the study

The goal of the article is to develop an algorithm on-line correction of the solar cell maximum power point tracking based on artificial network for photovoltaic electric power generation systems with increased efficiency due to intelligent control systems, made using an artificial neural network.

## 4. Materials and methods of research

### 4.1 How to create and train an artificial neural network

In recent decades, a new applied field of mathematics, specializing in artificial neural networks, has been developing rapidly. The relevance of research in this direction is confirmed by a lot of different applications of neural networks such as medical diagnostics or electric motor control [8, 9]. ANN has also been widely used in various solar panel studies. In its most general form, ANN simulates tasks or functions by performing calculations through learning. In the course of training, the network searches the training sample in a certain order. Browsing order can be sequential, random, etc. After training, the ANN acquires the ability to generalize and find reasonable exits when input is received data that does not occur during training [10]. The ability to learn is one of the main advantages of neural networks over conventional algorithms [11–14]. Technically, learning is about finding correlation ratios between neurons. ANN consists of simple processing units, neurons, and directional, weighted connections between these neurons. The connections between neurons are provided by synapses. The input information is multiplied by the corresponding connection strength - weight (synapse weight). The adder then adds signals coming from synaptic connections from the neurons of the previous layer. The last step in the calculation is the activation function through which the weighted amount passes. Further, the result is either passed to the next neuron with new weights, or is the network response. Today, there are many different configurations of neural networks with different operating principles that focus on a variety of tasks. In this work, a multi-layered direct distribution neural network was used, which is widely used to find patterns and classify images. The mathematical model of the neuron is described by the formula:

$$x_k^{(i+1)} = f \left( \sum_{j=1}^N w_j^{(k)} \cdot x_j^{(i)} \right) + B^{(k)}. \quad (1)$$

In Formula (1) the output of neuron of layer  $i+1$  is calculated as the weighted sum of all its inputs from layer  $i$ , to which the activation function normalizing the output signal is applied.

For this task, the artificial neural network has certain requirements: Accuracy and speed of operation, minimizing the number of neurons to facilitate subsequent implementation [15]. The classical method of artificial neural network creation includes several stages:

1. Data collection for training;
2. Production and optimization of data;
3. Selection of the network topology;

4. Selection of activation function;
5. Training and verification.

This technique has been improved and expanded to take into account the features of creating and configuring an artificial neural network to track the maximum power point. The improved synthesis consists of the following points:

1. Evaluation of the influence of external parameters on the solar battery and the system as a whole;
2. Selection of input and output parameters for the artificial neural network. At this stage, it is necessary to determine the place of ANN in the management system. This will determine the choice of the output parameter, the inputs for the ANN will be the parameters that have the strongest influence of the system;
3. Data collection for training. Both basic and supporting parameters;
4. Selection of network topology. Selection of ANN type, activation function, number of neurons in terms of required accuracy and implementation requirements;
5. Experimental modelling taking into account the selected network topology and prepared data for training;
6. Evaluation of the accuracy of the ANN operation, Verification of the operation of the artificial neural network on the test set and adjustment of the number of neurons;
7. Experimental simulation of ANN as part of the control system.

The information provided by the training sample generally determines the performance and efficiency of the ANN. In order to accomplish the task of tracking the solar battery's maximum power point, it is necessary to determine which parameters influence its characteristics, i.e. reflect the object patterns that the model must discover during the training [16]. The choice of parameters for learning artificial neural network and their processing is one of the most difficult and time-consuming steps of solving the problem. The training data set must meet several criteria:

1. The data shall reflect the true behavior of the object being examined;
2. Data should not be inconsistent.

The information provided by the training sample generally determines the performance and efficiency of the ANN. Experimental input was obtained from the Lucas-Nülle photovoltaic booth. The stand consists of a polycrystalline solar module and a halogen radiator, as a simulation of solar exploration. Tables 1 and 2 present the technical characteristics of the solar module and the halogen emitter.

**Table 1**

Solar Module Specification

Parameter	Significance
Voc (open circuit voltage)	21 V
Isc (short circuit current)	650 $\mu$ A
Maximum power	10 W

**Table 2**

Halogen radiator specification

Parameter	Significance
Mightiness	500 W
Mains voltage	230 V

Under laboratory conditions, the unit can simulate a maximum illumination level of 380 W/m<sup>2</sup>. For a more detailed analysis of the volt- and ampere characteristics, measurements were made in the light range of 95 to 380 W/m<sup>2</sup> and three temperatures of 20, 35 and 50 °C. The basic parameters of the solar battery reflect its volt-ampere and volt-watt characteristics. The volt-ampere characteristics for three levels of light and different temperatures are shown in Figures 1–4. In turn, the characteristics of the solar battery may be affected by environmental conditions such as radiation intensity (illumination), radiation angle and temperature. Since the radiation angle is somehow contained in the information about the value of illumination, this parameter can be ignored.

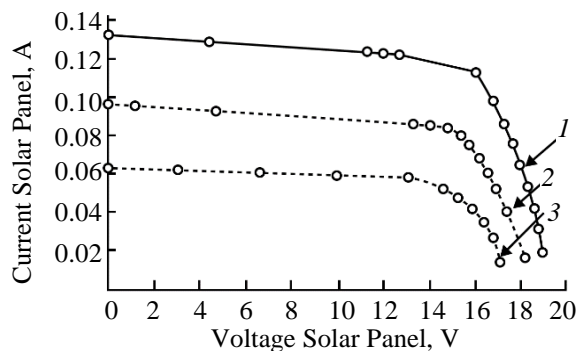


**Fig. 1.** Volt-ampere characteristics of the solar panel when changing illumination ( $T=35\text{ }^{\circ}\text{C}$ ):  
1 –  $380\text{ W/m}^2$ ; 2 –  $280\text{ W/m}^2$ ; 3 –  $180\text{ W/m}^2$

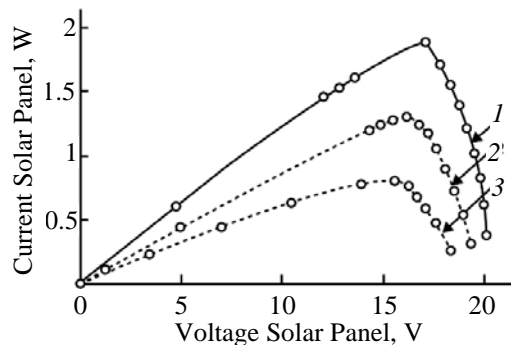


**Fig. 2.** Curves of the power of the solar panel when changing the light intensity ( $T=35\text{ }^{\circ}\text{C}$ ):  
1 –  $380\text{ W/m}^2$ ; 2 –  $280\text{ W/m}^2$ ; 3 –  $180\text{ W/m}^2$

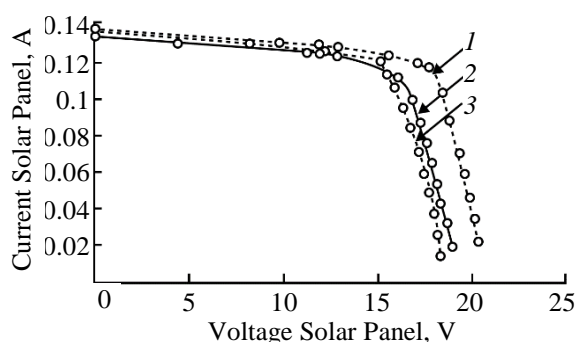


**Fig. 3.** Volt-ampere characteristics of the solar panel when changing temperature ( $E=380\text{ W/m}^2$ ):  
1 –  $20\text{ }^{\circ}\text{C}$ ; 2 –  $35\text{ }^{\circ}\text{C}$ ; 3 –  $50\text{ }^{\circ}\text{C}$

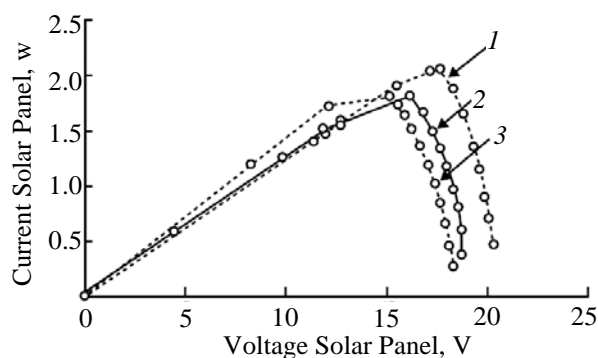


**Fig. 4.** Solar panel power curves when temperature changes ( $E=380\text{ W/m}^2$ ):  
1 –  $20\text{ }^{\circ}\text{C}$ ; 2 –  $35\text{ }^{\circ}\text{C}$ ; 3 –  $50\text{ }^{\circ}\text{C}$

Before operating a photovoltaic system, with a control system including an artificial neural network, it is necessary to adjust the network to the required parameters. Since the solar panels used to train the artificial neural network are likely to be different from the batteries it will have to operate with. Therefore, since the neural network has been trained in the laboratory to begin operation, it must be accompanied by online settings. The online correction of the artificial neural network is also linked to the problems of solar cell degradation.

#### 4.2 Degradation of solar panels

As a rule, photovoltaic stations are installed during the summer period and, in the case of the proposed maximum power point tracking algorithm, there is a primary neural network based on the original VSP simulated or laboratory conditions. A properly configured and trained system will work successfully until a certain time elapses and the characteristics of the solar battery will not change, i.e. until it starts to degrade. To this end, the control system must store tables of temperature, maximum power and voltage at the maximum power point. Despite the rapidly growing popularity of solar energy, producers and users face not only low efficiency but also degradation of photopanel.

It is common to distinguish two types of degradation of solar cells – natural degradation under the influence of solar radiation and degradation, Natural degradation, better known as Light Induced Degradation (LID) is a loss of performance due to solar radiation. This type of degradation can be explained by the fact that the silicon structure has traces of oxygen incorporated into the molten silicon during the Czochralski process. Under the action of light exposure, they can diffuse through the silicon grating and create complexes with acceptors of boron alloying impurity. Boro-oxygen complexes create their own energy levels in the silicon grating and can capture electrons and holes that are no longer involved in the photoeffect [17]. The average loss of capacity during the first year is usually regulated by the manufacturer and is about 3%. In the following years about 0.8%. The authors of article [18], an experiment was carried out, 58 modules of different manufacturers were exposed to intense solar radiation of  $25\text{ kWh/m}^2$  in 3 days. The experiment showed that about 57% of the modules

tested lost more than 3%. The second type of degradation when working at high voltage or Potential Induced Degradation (PID) – this type of degradation usually occurs when external potential is applied to the solar battery continuously, in the glass Na+ ions are generated, that create an electromagnetic field between the glass and the cell. Thus, slowly, after several months or years of operation in these conditions, the insulation layer weakens. Positive ions accumulate at the front of the cell creating localized short circuits. Conductive electrons present in the cell due to photoelectric effects flow from the cell to the metal frame. The metal frame is usually connected to the ground for safety reasons, so a small current leak is formed, and after a few months or years in these conditions the PID effect becomes macroscopic. No official PID statistics. Accredited laboratory Photovoltaik-Institut Berlin (PI Berlin) [19] published map. Data analysis has shown that PID occurs more frequently in climates with: high temperature, high humidity, high salt content in water, but also in continental areas (e.g., Central Germany) solar panels are also subject to PID. The authors of the article [20] argue that all known PID effects have one common characteristic: degradation depends on the polarity and level of potential between cell and ground. In order to better understand the cause of the PID-effect, the authors considered three levels of the solar battery – the system as a whole, the panel, the photocell. Having done this analysis, the authors concluded that despite the fact that the greatest impact is at the level of the photocell PID effect can be minimized and even avoided. The authors of article [21] examined and reviewed the work on the degradation of solar panels, as reported by various countries. The results were different, but on average about 1% per year. Since there are no official statistics on the effects of PID and the percentage of degradation can be any percentage, this study will only consider LID degradation (Light Induced Degradation).

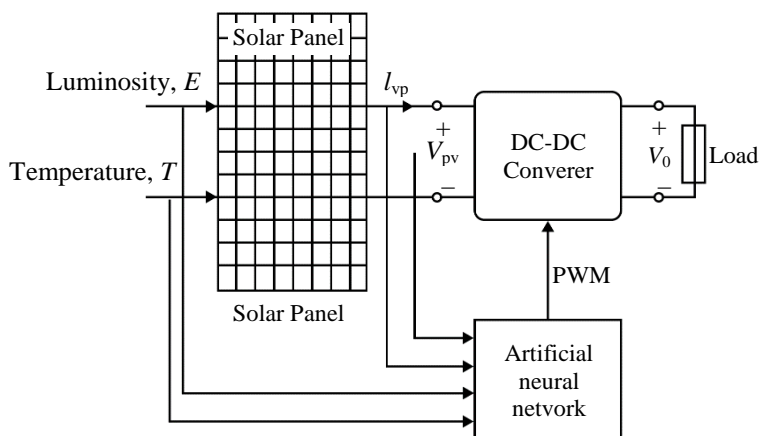


Fig. 5. Photovoltaic system flowchart with control algorithm neural network

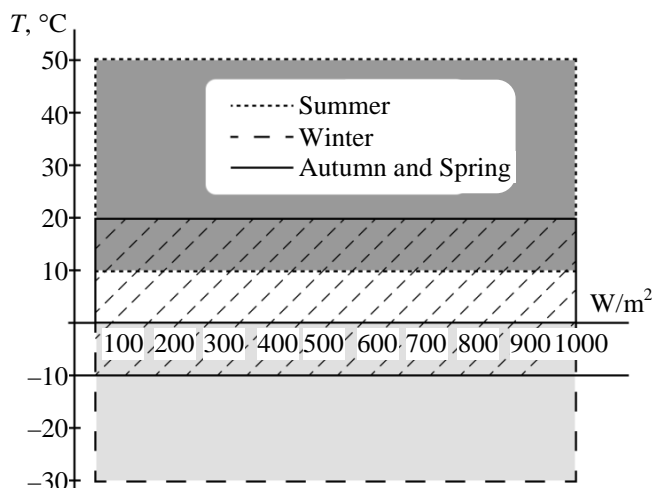


Fig. 6. Division of lighting unit and temperature into zones

### 4.3 Location of the neural network in the conversion system

The solar energy conversion system considered in this work is shown in Figure 5. The system consists of an array of solar panels, a three-port DC converter and a control system. The main component of the control system is the unit that operates the converter at the maximum power point. Tracking the maximum power point is a very important task when working with a solar energy converter. Since the function of tracking the maximum power point is performed by an artificial neural network, it will be investigated.

The data for the training were obtained by removing the volt-ampere characteristics of the solar module model at different light and temperature. Figure 6 shows the plane of light and temperature. Training data was divided by seasons, the boundaries of which are presented in Figure 6.

The neural network comprises an input layer, one hidden layer and one output. The network input data are: Temperature, voltage and current of the solar module. The output neuron signal is equal to the voltage at which the maximum power of the solar module is achieved.

#### 4.4 Online artificial neural network training

The experimental part of this article consists in the design, training, adjustment and subsequent adjustment of artificial neural network coefficients. When designing the ANN, the Elliott function was used as the activation function. The neural network was trained on data that included 100 volt-ampere characteristics in the light range from 10 to 1000 W/m<sup>2</sup> and temperatures from -30 to +50 °C. When designing an artificial neural network in real conditions, the light and temperature limits will change according to the climatic conditions of the region in question. The initial criterion for learning adequacy was the quadratic mean error (MSE). The results of several iterations of learning are shown in Table 7. Since the neural network will be updated each season and in order not to lose the precision of the work, we select the largest number of neurons in the hidden layer. The structure of the neural network is shown in Figure 7. Let's assume that the solar cell will deteriorate by 2% in one year. This is about 0.5% per season. Figure 8 shows, on a larger scale, the volt-wattage characteristics of the solar battery after degradation. As shown in Figure 8, after the degradation of the solar battery by 2%, the voltage at the maximum power point drops by 14 V, therefore, every year we will lose more power.

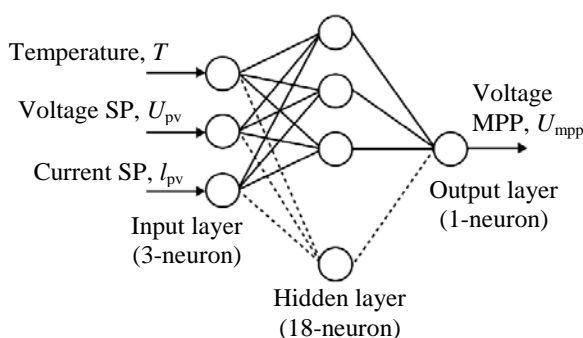


Fig. 7. Artificial neural network topology

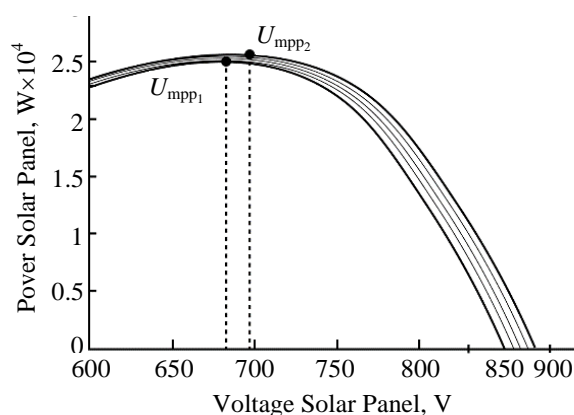


Fig. 8. Volt-Watt characteristics of solar battery degradation field

To avoid this problem, the artificial neural network needs to undergo additional learning after degradation. For this purpose, the calendar year was divided into zones where weather conditions, one way or another, repeat. As a rule, photovoltaic stations are installed during the summer period and, in the case of the proposed maximum power point tracking algorithm, there is a primary neural network based on the original VAC simulated or laboratory conditions. As mentioned earlier, the training array should cover all seasons by light and temperature. A properly configured and trained system will work successfully until a certain time elapses and the characteristics of the solar battery will not change, i.e. until it starts to degrade. For this purpose, the control system should store tables with temperature, maximum power and voltage values at the maximum power point (the table has a limited size equal to the number of VACs participating in the initial training). Next, when the system is in set mode, the control unit receives a command to compare the current temperature, maximum power and voltage at the optimum point.

If in the zone of a given season there is a line with the closest values of these parameters and the data on the optimum voltage have not been updated for a long time, the system goes into the mode of withdrawal of volt-ampere characteristic, which replaces previous values in the learning array to further form a new learning data array with subsequent online correction of artificial neural network coefficients. Such an experiment was carried out in Matlab software.

#### 4.5 Post-secondary education

In this experiment, the VAC of the degraded solar battery was removed and replaced at a time in the original learning table. Consequently, the new learning table included data on the behavior of the degraded solar battery in the current season and input data that stored information about other seasons. With a gradual degradation of 0.5% per season, we finish the ANN. Table 3 shows the average squared error for each season as the results against which learning adequacy can be assessed.

**Table 3**

Standard quadratic error for all calendar seasons

Season	Degradation	MSE
Summer	Initial	0.066
Fall	0.5%	1.3797
Winter	1%	1.3861
Spring	1.5%	5.4978
Summer	2%	1.0481

When designing an artificial neural network in real-world conditions, the light and temperature limits will vary according to the climatic conditions of the region in question. The initial criterion for learning adequacy was the mean quadratic error (MSE). The results of several training iterations are shown in Table 4.

**Table 4**

Selecting the number of neurons by average quadratic error

Number of neurons	MSE
8	0.0583
10	0.0267
12	0.0192
14	0.0173
16	0.0102
18	0.0066

In this version of online adjustment of artificial neural network coefficients, it can be noted that the accuracy of artificial neural network operation is reduced. The worst result is obtained in spring almost all the data has already been updated with a degradation of 1.5%, but ANN still stores the original data about the summer season, which differ significantly.

#### 4.6 Influence of Data Point Set of each VAC Solar Battery

In other words, a large number of points taken from a single volt-ampere characteristic greatly increases the size of the learning sample, which can lead to a decrease in the accuracy of the INS operation. Considering that not all VAC points are important for finding the maximum power point, it can be assumed that thinning in places of volt-ampere characteristic where the points are the most distant from the optimum point, will help to reduce the amount of data in the learning array and increase the importance of points in the maximum power point. The accuracy of ANN operation during the training is also affected by outdated data that the neural network still stores in its memory. It is therefore proposed to reduce their effect by thinning. In this case, outdated data will have little impact on the accuracy of the network after the degradation of the solar battery, but thinning will ensure adequate ANN operation outside the current season; Increasing the number of neurons to improve the accuracy of the artificial neural network can lead to retraining or require more examples in the learning sample. In order not to resort to increasing the number of neurons, improve accuracy and minimize the risk of re-training regularization is used:

$$E(w) = E_0(w) + \frac{\lambda}{2}[w^2] = \frac{1}{2} \sum_{i=1}^N (d_i - w^T x_i)^2 + \frac{\lambda}{2}[w^2]. \quad (2)$$

In formula (2):  $E_0(w)$  – function the regularization parameter, defined as the square of the expected errors, summed by N experimental routes in the medium;  $\lambda$  – Regularization is intended to prevent the retraining of the artificial neural network. This improves learning efficiency and results. More trained neurons gain more weight online.

#### 4.7 Seasonal learning with thinning

In this experiment, it is suggested that before online adjustment of the current season, a thinning of the training sample should be carried out. The preparation of the data for the online coefficient correction is as follows: the original data set needs to be thinned, to increase the importance of points near the maximum power point, i.e. the farther the current-voltage combination point on the VAC from the

maximum power point, the greater the chance that it will not get into the learning array (this thinning occurs with a fixed probability) This season's VAC replaces last year's data in the learning array, thus updating the learning array for the current degradation phase; next, the process of thinning the resulting learning data set with a certain probability to reduce the amount of data recorded with a different value of degradation and improve the accuracy of the neural network in the current season; then, we form a new learning sample by removing old data and adding a new season after degradation. All actions for each season are repeated after degradation. In this experiment, the thinning method was applied with varying probabilities simultaneously with regularization. Regularization varied from 1E-4 to 1E-9 for each degree of thinning. The results are presented in Tables 5-8. The best results for each season are highlighted in the tables in gray.

**Table 5**

Learning outcomes by autumn season

Reg. $\lambda$	Degree of thinning. Season – autumn							
	80	70	60	50	40	30	20	10
1E-4	1.58	1.43	2.65	1.78	1.76	1.58	1.67	2.77
1E-5	1.77	1.09	2.50	1.59	1.75	1.46	1.63	2.69
1E-6	1.27	0.88	2.39	1.45	1.62	1.27	1.58	2.63
1E-7	1.29	<b>0.74</b>	1.98	1.46	1.52	1.36	1.48	2.61
1E-8	1.19	0.77	2.48	1.41	1.40	1.12	1.48	2.53
1E-9	1.44	0.60	2.34	1.42	1.79	1.36	1.18	2.49

**Table 6**

Learning outcomes by winter season

Reg. $\lambda$	Degree of thinning. Season – winter							
	80	70	60	50	40	30	20	10
1E-4	0.32	1.43	0.64	1.31	1.19	1.71	1.16	1.62
1E-5	0.29	1.38	0.64	1.32	1.19	1.62	1.10	1.33
1E-6	0.23	1.21	0.48	0.42	1.03	1.32	1.01	1.19
1E-7	<b>0.18</b>	0.82	0.28	0.28	1.13	1.23	1.00	1.28
1E-8	0.21	0.93	0.45	0.31	1.12	1.12	1.02	1.27
1E-9	0.19	0.75	0.40	0.46	1.14	1.14	0.98	1.19

**Table 7**

Learning outcomes by spring season

Reg. $\lambda$	Degree of thinning. Season – spring							
	80	70	60	50	40	30	20	10
1E-4	0.58	1.64	0.76	2.21	1.78	8.86	3.97	5.78
1E-5	0.57	1.68	0.83	2.12	1.27	7.20	3.13	4.70
1E-6	0.37	0.82	0.65	1.31	1.17	6.51	3.25	4.79
1E-7	0.19	0.83	0.59	1.16	1.03	6.46	3.08	4.96
1E-8	0.26	1.11	0.49	1.09	1.08	7.14	2.81	4.96
1E-9	<b>0.21</b>	0.88	0.50	1.11	1.03	5.77	3.26	4.64

**Table 8**

Learning outcomes by summer season

Reg. $\lambda$	Degree of thinning. Season – summer							
	80	70	60	50	40	30	20	10
1E-4	0.74	0.94	1.01	1.68	1.13	1.71	1.39	1.43
1E-5	0.72	1.00	0.75	1.59	0.87	1.08	1.24	0.86
1E-6	0.71	0.66	0.78	1.28	0.83	1.19	1.14	0.79
1E-7	0.69	0.79	0.79	1.38	0.80	1.06	1.07	0.77
1E-8	0.66	0.91	0.77	1.28	0.72	1.11	1.05	0.68
1E-9	0.64	<b>0.58</b>	0.69	1.00	0.81	1.09	1.04	0.77

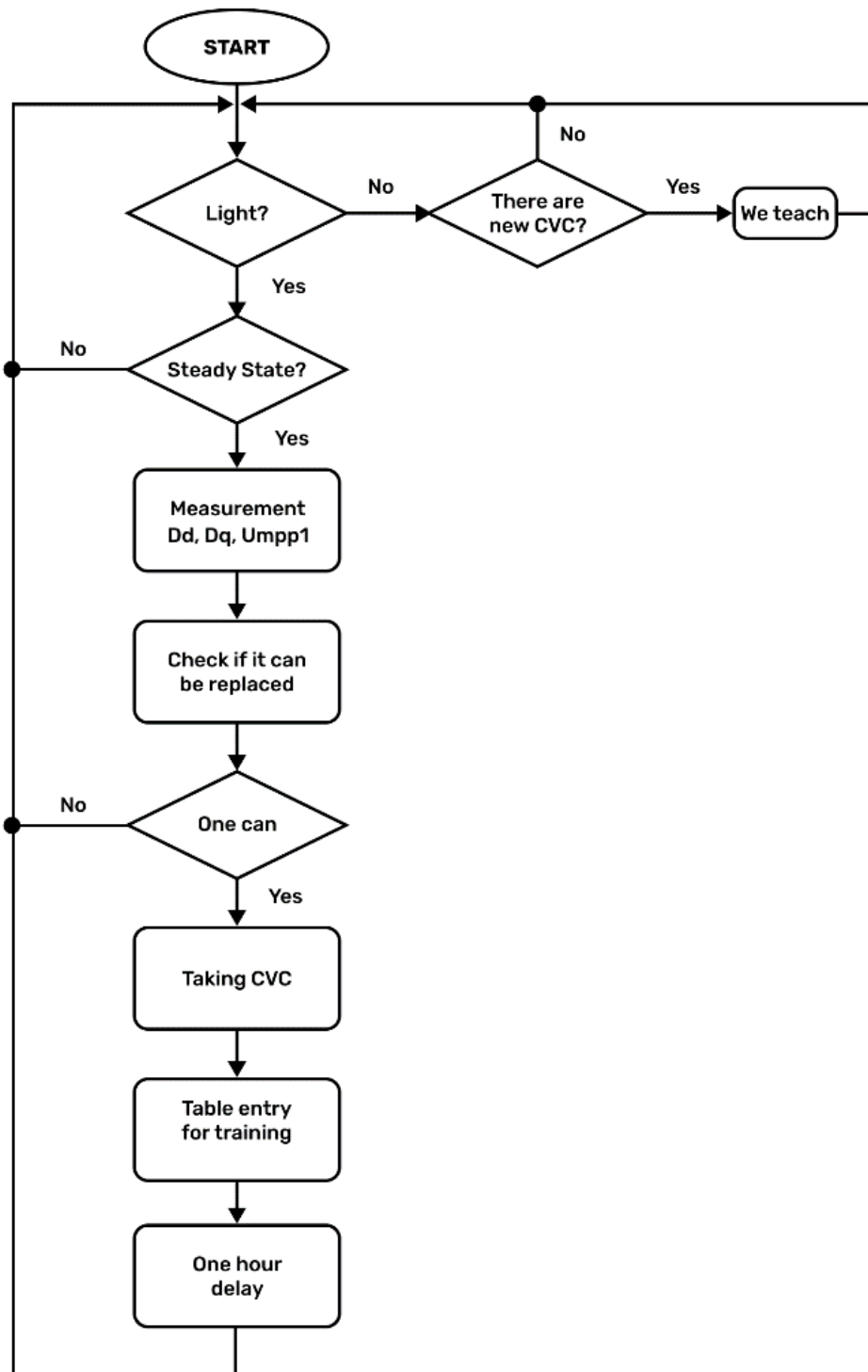


Fig. 9. Online Artificial Neural Network Coefficient Correction Flowchart

### 5. Result of research

On the basis of the results shown in the tables, we can conclude that the less old data left during retraining, the better the neural network is trained. Since the mean square error was counted on test data that were not part of the learning set, it can be observed that the regularization factor has no definite value. When designing the control system for the AC converter, a similar method of online correction of ANN coefficients will be used. The algorithm for the online correction of the coefficients of the artificial neural network will work according to the flowchart presented in Figure 9. The algorithm works as follows: To begin, the system must determine whether there is sufficient light, Next, when the system is in set mode, the control unit is commanded to measure d, q and voltage at the maximum

power point. If in the zone of a given season there is a line with the closest values of these parameters and the data on the optimum voltage have not been updated for a long time, the system goes into the mode of withdrawal of volt-ampere characteristic, which replaces the previous values in the learning array to further form a new learning data array followed by additional training. For an AC system, the algorithm will differ only in the number of artificial neural networks, a respectively, the number of parameters and tables that must be stored in the microprocessor memory.

## 6. Conclusions

The simulation showed, that an artificial neural network can be configured online to adjust the coefficients and perform well even when the parameters of a solar battery change. In order to optimize the accuracy of the artificial neural network, a new learning data set must be thinned out. This online INS coefficient correction algorithm can be applied not only to solar battery operation, but also to any other control system where the control object parameters change over time. It can also be noted that in this work the climatic zones were set in a simplified way, i.e., when setting up a real system, the climatic zones of a certain area in which the system will work should be defined and specified. The results may vary depending on the zone selected. With regard to artificial neural network learning, a simplified version was chosen where the neural network learns the new season across all VAC simultaneously. In real time, however, it can happen differently, for example once a week. That is, within a week, VAC data is collected and stored after the current degradation of the solar battery, and at the end of the week, the artificial neural network is set up online. In this case, the learning process may go differently and will differ from the results presented. As a result of this experiment, an algorithm for online correction of ANN coefficients was formed, which showed a good result and can be successfully used in modeling photoelectric generation systems.

## Литература

1. Technical photosynthesis involving CO<sub>2</sub> electrolysis and fermentation / T. Haas, R. Krause, R. Weber, M. Demler, and G. Schmid. *Nat. Catal.* 2018. vol. 1, № 1. P. 32–39.
2. Single-Junction Organic Solar Cell with over 15% Efficiency Using Fused-Ring Acceptor with Electron-Deficient Core / J. Yuan et al. *Joule*. 2019. vol. 3, № 4. P. 1140–1151.
3. 18% Efficiency organic solar cells / Q. Liu et al. *Sci. Bull.* 2020. vol. 65, № 2. P. 272–275.
4. Photocatalytic and Photoelectrochemical Systems: Similarities and Differences / H. Wu et al. *Adv. Mater.* 2020. vol. 32, № 18. P. 1904717. DOI: <https://doi.org/10.1002/adma.201904717>.
5. Organic and solution-processed tandem solar cells with 17.3% efficiency / L. Meng et al. *Science*. 2018. vol. 361, № 6407. P. 1094–1098.
6. Stable perovskite solar cells with efficiency exceeding 24.8% and 0.3-V voltage loss / M. Jeong et al. *Science*. 2020. vol. 369 (6511). P. 1615–1620. DOI: [10.1126/science.abb7167](https://doi.org/10.1126/science.abb7167).
7. Rahman M. W., Bathina C., Karthikeyan V., Prasanth R. Comparative analysis of developed incremental conductance (IC) and perturb observe (P&O) MPPT algorithm for photovoltaic applications. in *2016 10th International Conference on Intelligent Systems and Control (ISCO)*, Jan. 2016, pp. 1–6.
8. Ahmed J., Salam Z. A Modified P and O Maximum Power Point Tracking Method with Reduced Steady-State Oscillation and Improved Tracking Efficiency. *IEEE Trans. Sustain. Energy*. 2016. vol. 7, № 4. P. 1506–1515.
9. Development of an Improved P&O Algorithm Assisted Through a Colony of Foraging Ants for MPPT in PV System / K. Sundareswaran, V. Vigneshkumar, P. Sankar, S. P. Simon, P. Srinivasa Rao Nayak, and S. Palani. *IEEE Trans. Ind. Inform.* 2016. vol. 12, № 1. P. 187–200.
10. Koad R. B. A., Zobaa A. F., El-Shahat A. A Novel MPPT Algorithm Based on Particle Swarm Optimization for Photovoltaic Systems. *IEEE Trans. Sustain. Energy*. 2017. vol. 8, № 2. P. 468–476.
11. Papageorgiou E. I., Poczeta K. A two-stage model for time series prediction based on fuzzy cognitive maps and neural networks. *Neurocomputing*. 2017. vol. 232. P. 113–121.
12. Zhang N., Sutanto D., Muttaqi K. A review of topologies of three-port DC–DC converters for the integration of renewable energy and energy storage system. *Renew. Sustain. Energy Rev.* 2016. vol. 56. P. 388–401.
13. Arulmozhi Subramanian, Santha K.R. Review of multiport isolated bidirectional converter interfacing renewable and energy storage systems. *Int. J. Power Electron. Drive Syst. IJPEDS*. 2020. vol. 11, № 1. P. 466–476.
14. A call for quality. Power loss from crystalline module degradation causes a big headache for the industry. *PHOTON International*. 2018. P. 106–111.

15. Debije M. G., Verbunt P. P. C. Thirty years of luminescent solar concentrator research: Solar energy for the built environment. *Adv. Energy Mater.* vol. 2, № 1. P. 12–35. DOI: <https://doi.org/10.1002/aenm.201100554>.
16. Piegari L., Rizzo R., Spina I., Tricoli P. Optimized Adaptive Perturb and Observe Maximum Power Point Tracking Control for Photovoltaic Generation. *Energies*. 2015. vol. 8, № 5. P. 3418–3436.
17. Selvan S. Modeling and Simulation of Incremental Conductance MPPT Algorithm for Photovoltaic Applications. *Int. J. Sci. Eng. Technol.* 2013. vol. 2. P. 2277–1581.
18. Perturb and Observe MPPT algorithm with a current controller based on the sliding mode / E. Bianconi et al. *Int. J. Electr. Power Energy Syst.* 2013. vol. 1, № 44. P. 346–356.
19. Jordan D. C., Kurtz S. R. Photovoltaic Degradation Rates-an Analytical Review: Photovoltaic degradation rates. *Prog. Photovolt. Res. Appl.* 2013. vol. 21, № 1. P. 12–29.
20. Sutskever I., Martens J., Dahl G., Hinton G. On the importance of initialization and momentum in deep learning. *International Conference on Machine Learning*, Feb. 2013, pp. 1139–1147.
21. Farhat M. Photovoltaic Maximum Power Point Tracking Based on ANN Control. *Int. Rev. Model. Simul. IREMOS*. 2014. vol. 7. P. 114–120.

## References

1. T. Haas, R. Krause, R. Weber, M. Demler, & G. Schmid. (2018). Technical photosynthesis involving CO<sub>2</sub> electrolysis and fermentation, *Nat. Catal.*, 1, 1, 32–39.
2. J. Yuan et al. (2019). Single-Junction Organic Solar Cell with over 15% Efficiency Using Fused-Ring Acceptor with Electron-Deficient Core. *Joule*, 3, 4, 1140–1151.
3. Q. Liu et al. (2020). 18% Efficiency organic solar cells. *Sci. Bull.*, 65, 4, 272–275.
4. H. Wu et al. (2020). Photocatalytic and Photoelectrochemical Systems: Similarities and Differences. *Adv. Mater.*, 32, 18. 1904717. DOI: <https://doi.org/10.1002/adma.201904717>.
5. L. Meng et al. (2018). Organic and solution-processed tandem solar cells with 17.3% efficiency. *Science*, 361, 6407, 1094–1098.
6. M. Jeong et al. (2020). Stable perovskite solar cells with efficiency exceeding 24.8% and 0.3-V voltage loss. *Science*, 369, 6511. DOI: 10.1126/science.abb7167.
7. M. W. Rahman, C. Bathina, V. Karthikeyan, & R. Prasanth. (2016). Comparative analysis of developed incremental conductance (IC) and perturb observe (P&O) MPPT algorithm for photovoltaic applications. *2016 10th International Conference on Intelligent Systems and Control (ISCO)*, Jan. 2016, pp. 1–6.
8. Ahmed, J., & Salam Z. (2016). A Modified P and O Maximum Power Point Tracking Method with Reduced Steady-State Oscillation and Improved Tracking Efficiency. *IEEE Trans. Sustain. Energy*, 7, 4, 1506–1515.
9. K. Sundareswaran, V. Vigneshkumar, P. Sankar, S. P. Simon, P. Srinivasa Rao Nayak, & S. Palani. (2016). Development of an Improved P&O Algorithm Assisted Through a Colony of Foraging Ants for MPPT in PV System. *IEEE Trans. Ind. Inform.*, 12, 1, 187–200.
10. Koad, R. B. A., Zobia, A. F., & El-Shahat, A. (2017). A Novel MPPT Algorithm Based on Particle Swarm Optimization for Photovoltaic Systems. *IEEE Trans. Sustain. Energy*, 8, 2, 468–476.
11. Papageorgiou, E. I. & Poczeta, K. (2017). A two-stage model for time series prediction based on fuzzy cognitive maps and neural networks. *Neurocomputing*, 232, 113–121.
12. N. Zhang, D. Sutanto, & K. Muttaqi. (2016). A review of topologies of three-port DC–DC converters for the integration of renewable energy and energy storage system,” *Renew. Sustain. Energy Rev.*, 56, 388–401.
13. Arulmozhi, S., & Santha, K.R. (2020). Review of multiport isolated bidirectional converter interfacing renewable and energy storage systems. *Int. J. Power Electron. Drive Syst. IJPEDS*, 11, 1, 466–476.
14. A call for quality. Power loss from crystalline module degradation causes a big headache for the industry. (2018). *PHOTON International*, pp. 106–111.
15. M. G. Debije, & P. P. C. Verbunt. (2012). Thirty years of luminescent solar concentrator research: Solar energy for the built environment. *Adv. Energy Mater.*, 2, 1, 12–35.
16. L. Piegari, R. Rizzo, I. Spina, & P. Tricoli. (2015). Optimized Adaptive Perturb and Observe Maximum Power Point Tracking Control for Photovoltaic Generation. *Energies*, 8, 5, 3418–3436.
17. S. Selvan. (2013). Modeling and Simulation of Incremental Conductance MPPT Algorithm for Photovoltaic Applications. *Int. J. Sci. Eng. Technol.*, 2, 2277–1581.
18. E. Bianconi et al. (2013). Perturb and Observe MPPT algorithm with a current controller based on the sliding mode. *Int. J. Electr. Power Energy Syst.*, 1, 44, 346–356.
19. D. C. Jordan, & S. R. Kurtz. (2013). Photovoltaic Degradation Rates-an Analytical Review: Photovoltaic degradation rates. *Prog. Photovolt. Res. Appl.*, 21, 1, 12–29.

- 
20. I. Sutskever, J. Martens, G. Dahl, & G. Hinton. (2013). On the importance of initialization and momentum in deep learning. *International Conference on Machine Learning*, Feb. 2013, pp. 1139–1147.
21. M. Farhat. (2014). Photovoltaic Maximum Power Point Tracking Based on ANN Control. *Int. Rev. Model. Simul. IREMOS*, 7, 114–120.

**Тігарєв Володимир Михайлович**; Volodymyr Tigariiev, ORCID: 0000-0001-8492-6633

**Лопаків Олексій Сергійович**; Oleksii Lopakov, ORCID: 0000-0001-6307-8946

**Космачевський Володимир Володимирович**; Volodymyr Kosmachevskiy, ORCID: 0000-0002-3234-2297

**Андріанов Олександр Вікторович**; Oleksandr Andriianov, ORCID: 0000-0001-7037-0523

Received October 06, 2023

Accepted November 29, 2023